RHEOLOGICA ACTA

AN INTERNATIONAL JOURNAL OF RHEOLOGY

Vol. 17 | January/February 1978 | No. 1

Original Contributions · Originalarbeiten

Rheol. Acta **17**, 1–15 (1978)

ISSN 0035-4511/ASTM-Coden: RHEAAK

Meß- und Prüflaboratorium der BASF Aktiengesellschaft, Ludwigshafen am Rhein

Description of the non-linear shear behaviour of a low density polyethylene melt by means of an experimentally determined strain dependent memory function*)

H. M. Laun

With 12 figures and 3 tables

(Received July 12, 1977)

1. Introduction

The description of the nonlinear viscoelastic behaviour of polymer melts by means of an appropriate and mathematically simple constitutive equation is very helpful for the rheological characterization of polymer melts. The rheologist has to choose a set of tests which is sufficient to characterize the flow behaviour of a material rather completely. From these measurements he wants to predict the rheological behaviour of the melt at quite different flow situations. The constitutive equation is a guidance for the selection of the most suitable experiments for this characterization and makes is possible to calculate the material functions for a great variety of deformation histories.

During the last years many experiments have been performed to examine the applicability of a single integral constitutive equation given by *Lodge* (1, 2):

$$\sigma(t) + p\,\mathbf{1} = \int_0^\infty \mathring{\mu}(t-t')\,C^{-1}(t,t')\,d(t-t')\,. \qquad [1]$$

Here σ is the extra-stress tensor at the current time t, p the hydrostatic pressure, C^{-1} the Finger relative strain tensor between the states t and t', and $\mathring{\mu}$ is the memory function specific for the material. The zero superposed on symbols is used to distinguish the material functions describing the linear viscoelastic behaviour from those describing the nonlinear behaviour.

Recently a straightforward generalization of the rubberlike-liquid constitutive equation was proposed by *Wagner* (3, 4), where the memory function for the nonlinear behaviour $\mu(t-t'; I_1; I_2)$ is expressed as a product of the memory function for the linear behaviour $\mathring{\mu}(t-t')$ and a so-called damping function $h(I_1; I_2)$ depending on the first and second invariants of the Finger tensor:

$$\mu(t-t'; I_1; I_2) = \mathring{\mu}(t-t')\,h(I_1; I_2)\,. \qquad [2]$$

The aim of this paper is to give an experimental justification for assumption [2] and to show how the complete memory function describing the shear behaviour can directly be determined by rheological measurements. The predictions of the constitutive equation making use of the experimentally determined memory function are compared with measurements. It is important to test the predictions by means of quite different measuring quantities, as some material functions are rather insensitive to the special form of the memory function.

*) Paper presented at the Jahrestagung der DRG, Dortmund 1977.

2. Experimental

The shear flow data reported in this paper were obtained using a Weissenberg Rheogoniometer Model R 12/15 modified by *Meissner*. Details of the apparatus can be found in (5, 6). A cone angle of 8° was used. The plate diameters were 24 mm, 50 mm, and 72 mm. All measurements have been carried out on a stabilized LDPE melt formerly called 'Melt I' (7). The zero shear viscosity at $T = 150\,°C$ is $\eta_0 = 5.0 \times 10^4$ Pa s. An extensive series of rheological measurements on Melt I has been performed by *Meissner* (5, 6, 8, 12). The data already available from these measurements have been completed by additional experiments.

3. Linear viscoelastic behaviour

3.1. Time dependence

For simple shear flow the well known relations for the shear stress p_{12} and the primary normal-stress difference $p_{11} - p_{22}$

$$p_{12}(t) = \int_0^\infty \mathring{\mu}(t - t')\, \gamma_{t,t'}\, d(t - t')\,, \qquad [3]$$

$$[p_{11} - p_{22}](t) = \int_0^\infty \mathring{\mu}(t - t')\, \gamma_{t,t'}^2\, d(t - t') \qquad [4]$$

are obtained from eq. [1] (1). Here $\gamma_{t,t'}$ is the relative shear strain between the states t' and t. It is convenient to approximate the memory function by a sum of exponential functions with time constants τ_i and coefficients a_i (9, 2):

$$\mathring{\mu}(t - t') = \sum_i a_i \exp\left[-\frac{t - t'}{\tau_i}\right]. \qquad [5]$$

Using [5], for oscillatory shear flow of angular frequency ω the following expressions for the storage modulus $\mathring{G}'(\omega)$ and the loss modulus $\mathring{G}''(\omega)$ are derived from [3]:

$$\mathring{G}'(\omega) = \sum_i a_i \tau_i \frac{\omega^2 \tau_i^2}{1 + \omega^2 \tau_i^2}\,, \qquad [6]$$

$$\mathring{G}''(\omega) = \sum_i a_i \tau_i \frac{\omega \tau_i}{1 + \omega^2 \tau_i^2}\,. \qquad [7]$$

To each relaxation time τ_i a relaxation strength $g_i = a_i \cdot \tau_i$ is attributed. Figure 1 shows measurements of $\mathring{G}'(\omega)$ and $\mathring{G}''(\omega)$ performed by *Zosel* (10). The moduli measured at different temperatures are plotted as functions of the reduced angular frequency $a_T\omega$ to get master curves at a reference temperature of $T_0 = 150\,°C$ (11), a_T being the shift factor. For the approximation of the memory function eight relaxation times τ_i between 10^{-4} s and 10^3 s with decimal

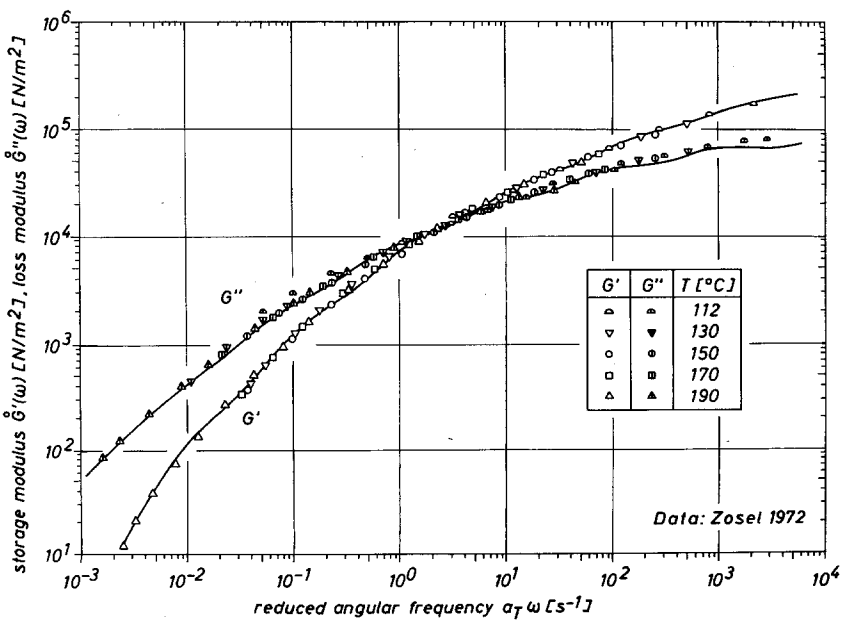

Fig. 1. Shear moduli of LDPE Melt I as functions of the reduced angular frequency. Reference temperature $T_0 = 150\,°C$. The full lines were calculated according to [6] and [7] using the constants of table 1

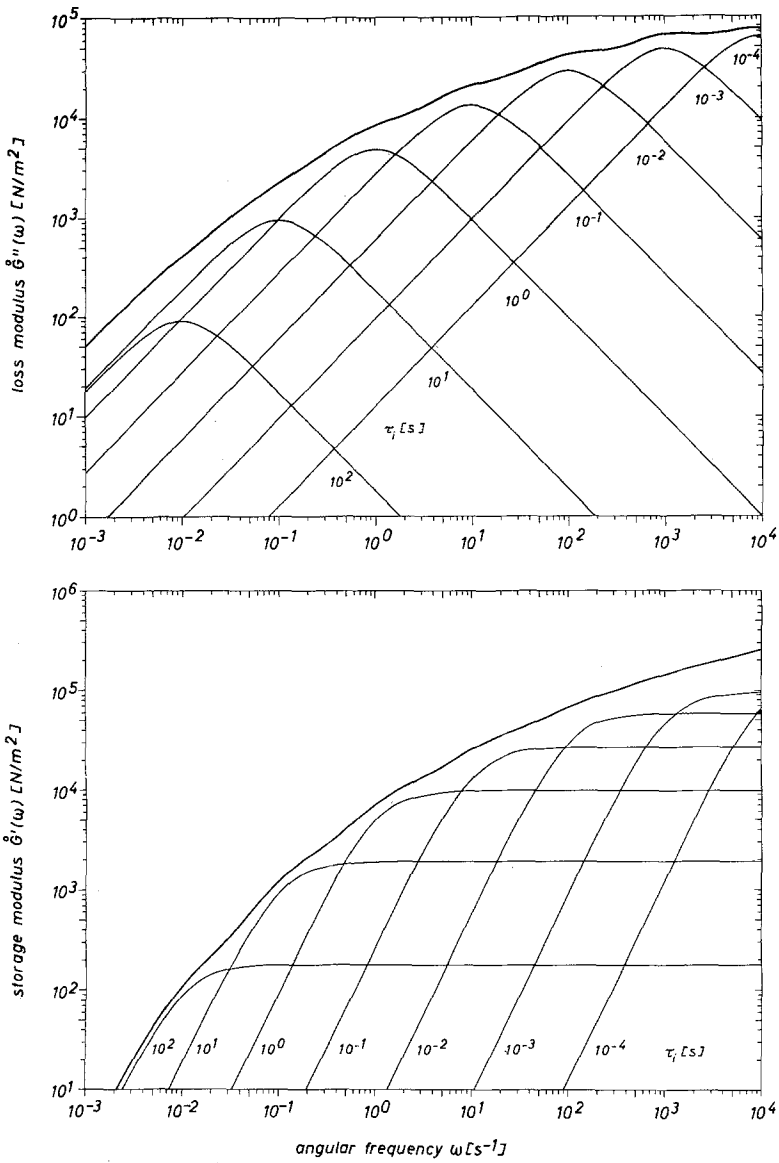

Fig. 2. Frequency dependence of the shear moduli at $T = 150\,°C$ as represented by a sum of eight terms with decimal spacing of the time constants τ_i. The contribution of the term with $\tau_i = 10^3$ s is not seen in the diagramm

Table 1. Set of constants used to describe the time dependence of the linear viscoelastic behaviour of Melt I at $T_0 = 150\,°C$ according to eq. [5]

i	τ_i[s]	a_i[N m^{-2} s^{-1}]
1	10^3	1.00×10^{-3}
2	10^2	1.80×10^{0}
3	10^1	1.89×10^{2}
4	10^0	9.80×10^{3}
5	10^{-1}	2.67×10^{5}
6	10^{-2}	5.86×10^{6}
7	10^{-3}	9.48×10^{7}
8	10^{-4}	1.29×10^{9}

spacing have been chosen. The coefficients a_i were determined by a fit of [6] and [7] to the data in fig. 1 [1]). Table 1 gives the set of constants which was used to describe $\mathring{\mu}(t-t')$ at $T_0 = 150\,°C$. The moduli calculated with these constants are drawn as full lines in figure 1. It is seen that the choice of a discrete relaxation spectrum with decimal spacing of the relaxation

[1]) From $\mathring{G}'(\omega)$ and $\mathring{G}''(\omega)$ separate sets of coefficients can be obtained which should be identical within experimental error.

times may lead to non-monotonous material functions. This is illustrated by figure 2 where the contributions of each term of the series to the moduli are shown. Another disadvantage of the series representation of the memory function is the fact that the relaxation strengths g_i have no direct physical meaning, because the choice of the τ_i is arbitrary. However, this representation makes it possible to describe the linear viscoelastic behaviour over a wide range of time scale by means of only a few constants. The integration of eqs. [3] and [4] is simplified and the contribution of each relaxation time to the material functions can easily be surveyed.

In the linear viscoelastic range the shear relaxation modulus $\mathring{G}(t)$ after a step in shear strain γ_0 is given by

$$\mathring{G}(t) = \frac{p_{12}(t)}{\gamma_0} = \sum_i a_i \tau_i \exp\left[-\frac{t}{\tau_i}\right]. \qquad [8]$$

A comparison of the shear relaxation modulus calculated by means of [8] using the coefficients of table 1 with measurements of *Meissner* (5) is shown in figure 3. The weak oscillation of the predicted $\mathring{G}(t)$ is caused by the use of a discrete relaxation spectrum, as discussed above. It is obvious that the experimental behaviour is well described by the calculated function if these oscillations are smoothed.

In figure 4 the calculated and measured stress growth at the onset of steady shear flow are compared. The stressing viscosity $\mathring{\eta}(t)$ for a shear rate $\dot{\gamma}_0$ in the linear viscoelastic range was calculated by

$$\mathring{\eta}(t) = \frac{p_{12}(t)}{\dot{\gamma}_0} = \sum_i a_i \tau_i^2 \left(1 - \exp\left[-\frac{t}{\tau_i}\right]\right). \qquad [9]$$

For $t > 0.5$ s the agreement between the calculated curve and the experimental data is convincing. However, at short times the measured values show a delay in time compared with the predicted behaviour [2]).

[2]) The rotation of the upper plate of the rheogoniometer was taken into account by the servo control of the apparatus (6). The discrepancy is probably due to the limited performance of the apparatus at short times. This is why measurements of the stress growth in the linear viscoelastic range are not recommendable for the determination of the coefficients a_i for relaxation times $\tau_i \ll 0.5$ s. Furthermore, only a poor accuracy of the coefficients can be expected for the long relaxation times because the stressing viscosity reaches a steady-state value as function of time.

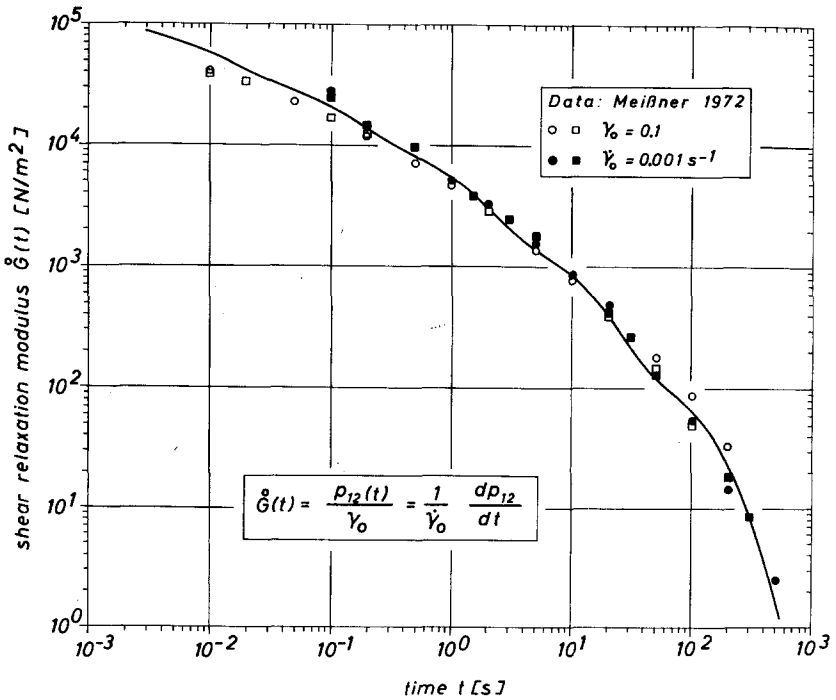

Fig. 3. Time dependence of the shear relaxation modulus in the linear viscoelastic range at $T = 150$ °C. (○ □) measured after a step in shear strain of $\gamma_0 = 0.1$, (● ■) calculated from the relaxation of shear stress after stop of steady shear flow at a shear rate of $\dot{\gamma}_0 = 10^{-3}\ s^{-1}$ according to the formula in the figure (5). (——) calculated according to eq. [8] using the constants of table 1

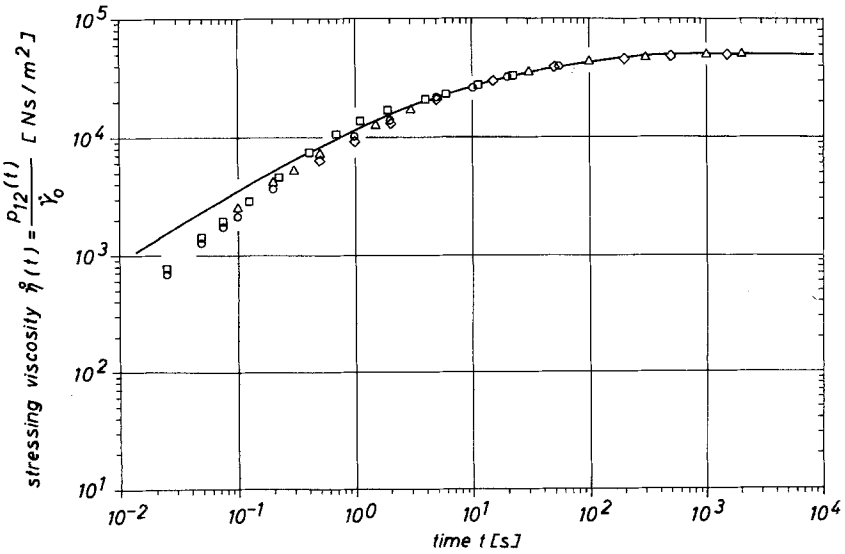

Fig. 4. Time dependence of the stressing viscosity in the linear viscoelastic range at $T = 150\,°C$ measured at a shear rate of $\dot{\gamma}_0 = 10^{-3}\,s^{-1}$. The full line was calculated according to eq. [9] using the constants of table 1

3.2. Temperature dependence

Polyethylene melts are thermo-rheologically simple fluids. This means that a variation of temperature corresponds to a shift in time scale (13, 11, 19). Accordingly all relaxation times change with temperature proportional to the shift factor a_T

$$\tau_i(T) = a_T \tau_i(T_0)\,. \qquad [10]$$

The relaxation strengths g_i remain constant (11), from which it follows that

$$a_i(T) = \frac{1}{a_T}\, a_i(T_0)\,. \qquad [11]$$

The shift factor is determined by the temperature dependence of the zero shear viscosity η_0:

$$a_T(T) = \frac{\eta_0(T)}{\eta_0(T_0)} = \exp\left[\frac{E_0}{R}\left(\frac{1}{T} - \frac{1}{T_0}\right)\right]. \qquad [12]$$

For the LDPE melt investigated the activation energy is $E_0 = 13\,\text{kcal/Mol} = 54\,\text{kJ/Mol}$ (12). By the set of constants $a_i(T_0)$, $\tau_i(T_0)$ for the reference temperature T_0 (table 1) and the temperature dependence $a_T(T)$ of the shift factor (eq. [12]) the memory function of Melt I for the linear viscoelastic behaviour is completely determined.

4. Memory function for the nonlinear viscoelastic behaviour

4.1. Strain and time dependence

According to *Wagner* (3, 4) for simple shear flow the generalized memory function is expressed by

$$\mu(t - t'; \gamma_{t,t'}) = \mathring{\mu}(t - t')\, h(\gamma_{t,t'})\,. \qquad [13]$$

As only the shear behaviour is regarded the invariants of the Finger relative strain tensor $I_1 = I_2 = \gamma_{t,t'}^2 + 3$ are replaced by $\gamma_{t,t'}$. Eq. [13] represents a special case of the BKZ model (24). The nonlinearity of the rheological behaviour is only characterized by the damping function $h(\gamma_{t,t'})$. For $h(\gamma_{t,t'}) = 1$ the melt behaves linear viscoelastic. In this case the memory function is only time dependent. In the nonlinear viscoelastic range $h(\gamma_{t,t'}) < 1$ is valid, and the memory function becomes strain dependent.

Eq. [13] can experimentally be checked by applying a step γ_0 in shear strain defined by

$$\gamma_{t,t'} = \begin{cases} 0 & \text{for} \quad t - t' < t \\ \gamma_0 & \text{for} \quad t - t' \geq t \end{cases} \qquad [14]$$

and measuring the resulting stresses. Using [13], [14], and [3] one gets for the shear relaxation modulus $G(t; \gamma_0)$ which describes the relaxation of the shear stress p_{12}

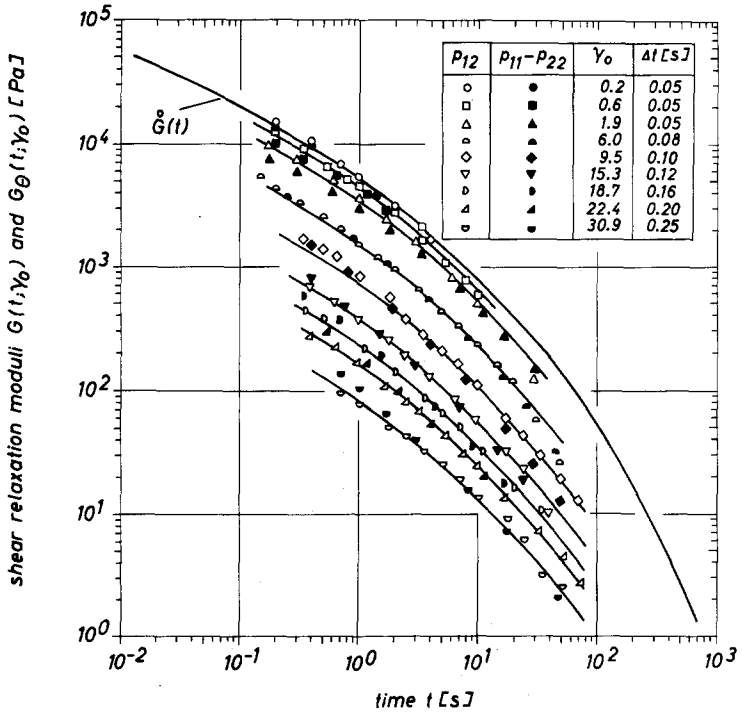

Fig. 5. Time dependence of the shear relaxation moduli determined from the relaxation of the shear stress and primary normal stress difference at $T = 150\,°C$ and different shear strains γ_0. The rise time for the step was Δt. The influence of the non-zero rise time was taken into account as described in the appendix

$$G(t;\gamma_0) = \frac{p_{12}(t)}{\gamma_0} = \frac{1}{\gamma_0}\int_t^\infty \dot{\mu}(t-t')\,h(\gamma_0)\,\gamma_0\,d(t-t') = \mathring{G}(t)\,h(\gamma_0)\,. \quad [15]$$

The relaxation of the primary normal stress difference is described by the modulus $G_\Theta(t;\gamma_0)$. Using [13], [14], and [4] one obtains

$$G_\Theta(t;\gamma_0) = \frac{[p_{11}-p_{22}](t)}{\gamma_0^2} = \frac{1}{\gamma_0^2}\int_t^\infty \dot{\mu}(t-t')\,h(\gamma_0)\,\gamma_0^2\,d(t-t') = \mathring{G}(t)\,h(\gamma_0)\,. \quad [16]$$

According to [15] the time dependence of $G(t;\gamma_0)$ remains uneffected by a variation of γ_0 but the amount of the modulus decreases proportional to $h(\gamma_0)$. This relation has been used by *Osaki* (14, 15) to determine the damping functions of polymer solutions. By comparing [15] and [16] it is seen that the moduli determined from the relaxation of the shear stress and from the relaxation of the primary normal stress difference are identical: $G_\Theta(t;\gamma_0) = G(t;\gamma_0)$.

Measurements of the relaxation moduli[3]) were performed up to a shear strain of $\gamma_0 = 30.9$ where the melt behaves strongly nonlinear (fig. 5). The shear relaxation modulus $\mathring{G}(t)$ for the linear viscoelastic behaviour which is represented in figure 5 as full line corresponds to eq. [8] and figure 3 after smoothing of the oszillations. The full lines connecting the points measured at different shear strains γ_0 have been obtained by shifting the curve $\mathring{G}(t)$ along the modulus axis. This means that the time dependence of the relaxation moduli remains unaffected by γ_0 although their absolute values decrease by two decades. Moreover, figure 5 shows the agreement between $G_\Theta(t;\gamma_0)$ and $G(t;\gamma_0)$.

[3]) It has been tried to minimize the rise time Δt for the step γ_0 but to accomplish it at a constant shear rate $\dot{\gamma}_0 = \gamma_0/\Delta t$. The reason for this is that the error in $G(t;\gamma_0)$ and $G_\Theta(t;\gamma_0)$ due to the non-zero rise time can then be estimated by means of the constitutive equation. The error has been taken into account as described in detail in the appendix.

A plot of $G(t;\gamma_0)/\mathring{G}(t)$ as a function of γ_0 for an arbitrarily chosen time $t = t^*$ directly represents the strain dependence of the relaxation modulus or as a consequence of [15] the damping function $h(\gamma_0)$. This analysis was carried out for $t^* = 3$ s (fig. 6). For the approximation of the damping function a single exponential function

$$h(\gamma_0) = \exp[-n\gamma_0] \qquad [17]$$

with only one parameter $n = 0.143$ has been proposed by *Wagner* (13) for Melt I. We have determined $n = 0.18$ by a best fit of the viscosity function (see eq. [27]) using the constants of table 1. In figure 6 function [17] for $n = 0.18$ is represented by a broken line. The single exponential damping function gives a good description of the experimental results up to $\gamma_0 \approx 13$.

For higher shear strains the predicted values are too small compared with the measurements.

A better description of the experimental data in figure 6 is obtained by a damping function, as proposed by *Osaki* (14), which is represented by a sum of two exponential functions

$$h(\gamma_0) = f_1 \exp[-n_1\gamma_0] + f_2 \exp[-n_2\gamma_0]. \qquad [18]$$

This damping function is characterized by three parameters n_1, n_2, and f_1 as $f_2 = 1 - f_1$. A fit of the parameters to the data in figure 6 yields the full line. The constants obtained are listed in table 2. It is seen from figure 6 that the description of the experimentally determined damping function by eq. [18] is very satisfactory.

Table 2. Set of constants used to describe the damping functions according to eqs. [17] and [18]

damping function	f_1	n_1	f_2	n_2
$\exp[-n\gamma_{t,t'}]$	1	0.18	–	–
$f_1 \exp[-n_1\gamma_{t,t'}] + f_2 \exp[-n_2\gamma_{t,t'}]$	0.57	0.310	0.43	0.106

4.2. Temperature dependence

It has been found by several authors that temperature invariant master curves can be obtained even for nonlinear material functions, e.g. the viscosity function (16, 17). This requires that the damping function is independent of temperature, i.e.

$$h(\gamma_0; T) = h(\gamma_0; T_0). \qquad [19]$$

From the temperature invariance of the damping function it follows that the influence of the temperature on the nonlinear shear behaviour can be described by the shift factor a_T like it has been found for the linear viscoelastic

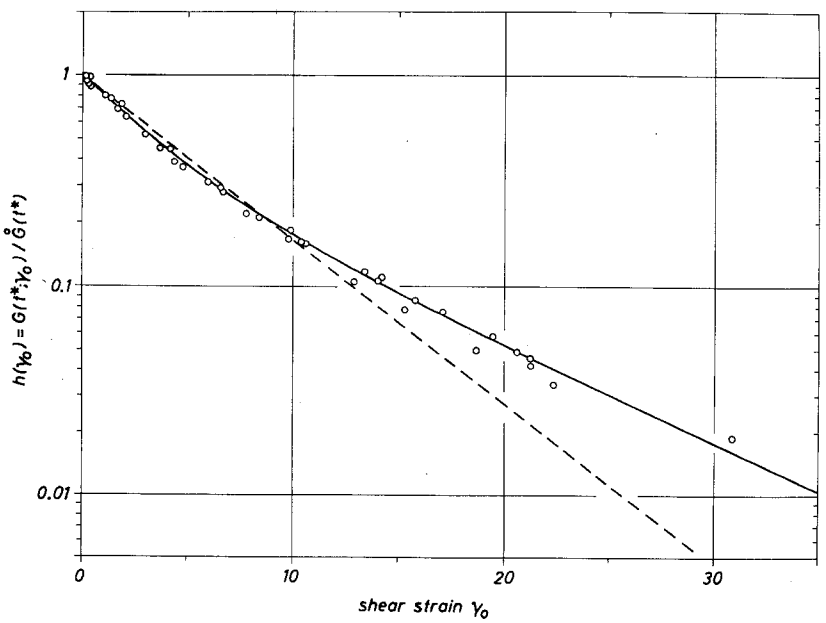

Fig. 6. Shear strain dependence of the damping function as determined by shear relaxation modulus measurements at $T = 150$ °C and $t^* = 3$ s. The full line corresponds to eq. [18] using the constants of table 2. The broken line represents the single exponential damping function [17]

behaviour. Table 3 gives a comparison of the values $h(\gamma_0; T)$ measured at three different

Table 3. Temperature dependence of the damping function as determined by shear relaxation modulus measurements

T[°C]	120	150	210
γ_0		$h(\gamma_0)$	
5	0.31	0.37	0.29
10	0.14	0.17	0.16
15	0.066	0.093	0.090
20	0.034	0.052	0.056

temperatures. The data at 150 °C are taken from figure 6, the data at 120 °C and 210 °C are preliminary results. The values for small γ_0 are quite similar whereas the results obtained at 120 °C and high γ_0 differ considerably from those measured at 150 °C [4]).

Knowing the damping function at the reference temperature T_0 the complete memory function for the shear behaviour of Melt I is determined. The time dependence of the memory function is described by $\hat{\mu}(t-t')$, the temperature dependence by $a_T(T)$, and the strain dependence by $h(\gamma_{t,t'})$. Each of these functions is approximated by exponential functions characterized by a set of constants which were experimentally determined. The constitutive equation can now be applied to predict the nonlinear shear behaviour of Melt I for quite different shear histories. This is shown for some important material functions which can be calculated by closed integration [5]). The predicted material functions, valid at the reference temperature of $T_0 = 150$ °C, are compared with measurements. The temperature dependence of the rheological behaviour is taken into account by temperature invariant plots of the measured material functions.

5. Calculation of nonlinear material functions

For Wagner's damping function $h(\gamma_{t,t'}) = \exp[-n\gamma_{t,t'}]$ the following relations are obtained [6]):

$$p_{12}(t) = \sum_i a_i \int_{t-t'=0}^{\infty} \exp\left[-\frac{t-t'}{\tau_i}\right] \cdot \exp[-n\gamma_{t,t'}]\,\gamma_{t,t'}\,d(t-t'), \quad [20]$$

$$[p_{11}-p_{22}](t) = \sum_i a_i \int_{t-t'=0}^{\infty} \exp\left[-\frac{t-t'}{\tau_i}\right] \cdot \exp[-n\gamma_{t,t'}]\,\gamma_{t,t'}^2\,d(t-t'). \quad [21]$$

The time dependence of the shear stress and primary normal stress difference calculated for the single exponential damping function can easily be generalized for a damping function represented by a sum of exponential functions $h(\gamma_{t,t'}) = f_1 \exp[-n_1\gamma_{t,t'}] + f_2 \exp[-n_2\gamma_{t,t'}]$ simply by a linear superposition. For the shear stress we get

$$p_{12}(t; n) \to f_1 p_{12}(t; n_1) + f_2 p_{12}(t; n_2). \quad [22]$$

The same is true for the primary normal stress difference. Thus we can restrict the calculations to the single exponential damping function.

5.1. Stress growth after the sudden imposition of a constant shear rate $\dot{\gamma}_0$

The shear history is defined by

$$\gamma_{t,t'} = \begin{cases} \dot{\gamma}_0(t-t') & \text{for} \quad t-t' < t \\ \dot{\gamma}_0 t & \text{for} \quad t-t' \geq t. \end{cases} \quad [23]$$

On substituting $\gamma_{t,t'}$ in [20] and [21] we can calculate the stressing viscosity $\eta(t;\dot{\gamma}_0)$ and the primary normal stress coefficient $\Theta(t;\dot{\gamma}_0)$ by closed integration:

$$\eta(t;\dot{\gamma}_0) = \frac{p_{12}(t;\dot{\gamma}_0)}{\dot{\gamma}_0} = \sum_i \frac{a_i\tau_i^2}{(1+n\dot{\gamma}_0\tau_i)^2} \cdot \{1-\exp[-t_{r,i}](1-n\dot{\gamma}_0\tau_i t_{r,i})\}, \quad [24]$$

$$\Theta(t;\dot{\gamma}_0) = \frac{[p_{11}-p_{22}](t\ \dot{\gamma}_0)}{\dot{\gamma}_0^2} = 2\sum_i \frac{a_i\tau_i^3}{(1+n\dot{\gamma}_0\tau_i)^3} \cdot \left\{1-\exp[-t_{r,i}] \cdot \left(1+t_{r,i}-\frac{n\dot{\gamma}_0\tau_i}{2}t_{r,i}^2\right)\right\}. \quad [25]$$

[4]) The discrepancy at 120 °C is probably due to edge effects in the cone-and-plate gap and an adiabatic heating of the melt as the shear rates $\gamma_0/\Delta t$ at this temperature were the highest compared with the strain rates at which the melt behaves linear viscoelastic.

[5]) A comparison of the predicted shear creep and recovery behaviour of Melt I with measurements may be found in (19).

[6]) Eqs. [20] and [21] are equivalent to those obtained by *Phillips* (22) by introducing a new strain measure $\gamma_{t,t'}\exp[-n\gamma_{t,t'}]$ instead of a strain dependent memory function.

The reduced time $t_{r,i}$ stands for

$$t_{r,i} = t/\tau_i + n\dot{\gamma}_0 t\,. \qquad [26]$$

It is noteworthy that the time dependent terms on the right hand sides of eqs. [24] and [25] are multiplied by the factors $\exp[-t_{r,i}]$. From this it follows that a steady-state shear viscosity η_s and a steady-state primary normal-stress coefficient Θ_s, respectively,

$$\eta_s(\dot{\gamma}_0) = \sum_i \frac{a_i \tau_i^2}{(1 + n\dot{\gamma}_0 \tau_i)^2}\,, \qquad [27]$$

$$\Theta_s(\dot{\gamma}_0) = 2\sum_i \frac{a_i \tau_i^3}{1 + n\dot{\gamma}_0 \tau_i^3} \qquad [28]$$

are obtained for $t_{r,i} \gg 1$. At small shear rates this is only true for $t \gg \tau_{i,\max}$, $\tau_{i,\max}$ being the longest relaxation time of the memory function $\mathring{\mu}(t - t')$, whereas at high shear rates even for $t \ll \tau_{i,\max}$ a steady-state is reached if for the magnitude of shear $\dot{\gamma}_0 t \gg 1/n$ is valid.

The viscosity function $\eta_s(\dot{\gamma}_0)$ and the primary normal-stress function $\Theta_s(\dot{\gamma}_0)$ as calculated according to eqs. [27] and [28] are compared with experimental data in figure 7. The reduced viscosities and primary normal stress coefficients η_s/a_T and Θ_s/a_T^2, respectively, are plotted as functions of the reduced shear rate $a_T\dot{\gamma}_0$. The material functions calculated by using the experimentally determined damping function are represented by full lines, those calculated by using the single exponential damping function by broken lines. The viscosity functions predicted by means of both damping functions cannot be distinguished within the accuracy of the graph. The values for Θ_s are more sensitive to the special form of the damping function.

The agreement between the calculated material functions and the measurements is very satisfactory. It should be pointed out that η_s and Θ_s are predicted by means of a memory function which has been determined by measuring quite different quantities, namely the frequency dependence of the complex shear modulus $G^*(\omega)$ and the strain dependence of the shear relaxation modulus $G(t;\gamma_0)$. In order to compute the viscosity function for a wide range of shear rates it is necessary according to

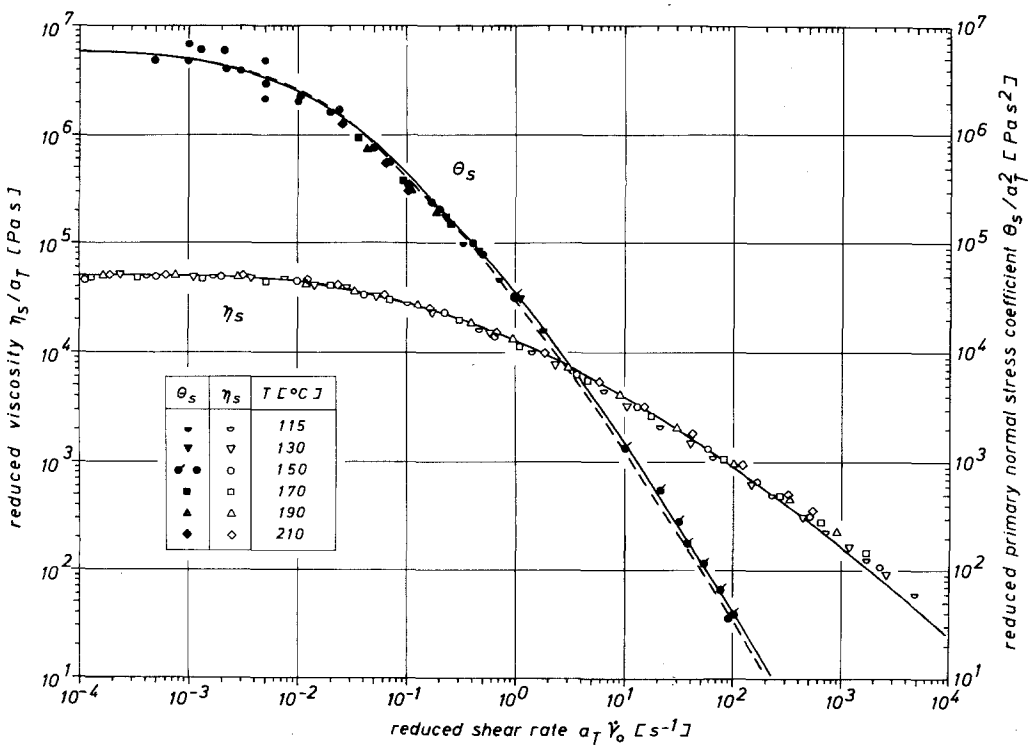

Fig. 7. Temperature invariant representation of the steady-state viscosity (12) and steady-state primary normal stress coefficient as functions of the reduced shear rate. Reference temperature $T_0 = 150\,°C$. The viscosities at high shear rates were obtained by a capillary rheometer. The tic denotes measurements with a modified gap geometry similar to that used in (23). (——) prediction of [27] and [28] using the experimentally determined damping function. (– – –) calculated by means of the single exponential damping function

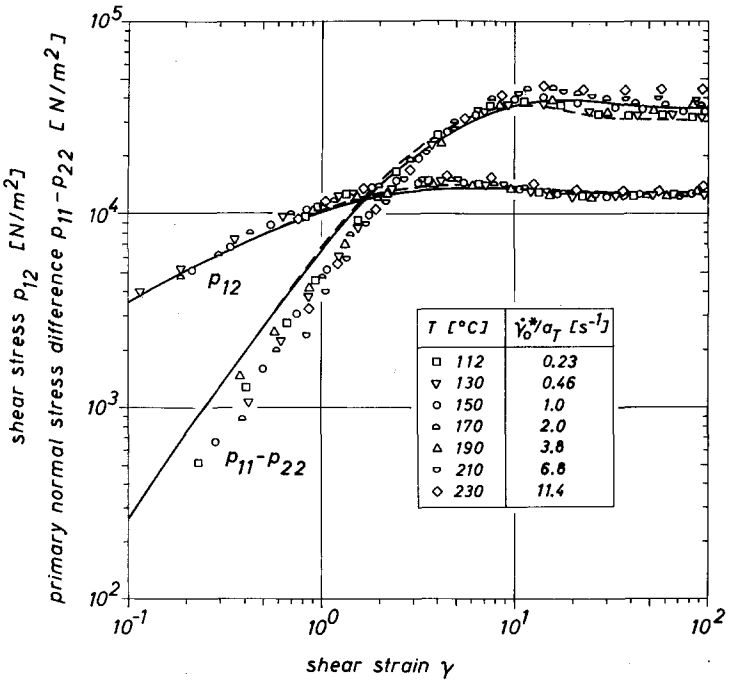

Fig. 8. Temperature invariant representation of the shear stress and primary normal stress difference as function of shear strain in stressing tests. The shear rate was $\dot{\gamma}_0^* = 1\ s^{-1}$ at the reference temperature of $T_0 = 150\,°C$. (——) prediction using [18], (– – –) prediction using the single exponential damping function

[27] to determine the memory function $\mathring{\mu}(t-t')$ over a correspondingly large range of time scale.

The time dependence of the shear stress and the primary normal-stress difference in stressing tests as given by [24] and [25], respectively, are compared with measurements in figure 8. Both quantities are plotted versus shear strain $\gamma = \dot{\gamma}_0 t$ in order to obtain a temperature invariant representation of the predicted behaviour. The shear rate is $\dot{\gamma}_0 = \dot{\gamma}_0^* = 1\ s^{-1}$ at the reference temperature of $T_0 = 150\,°C$. As discussed above, a variation of temperature corresponds to a shift in time scale. Therefore, the measurements at different temperatures were performed at corresponding shear rates $\dot{\gamma}_0 = \dot{\gamma}_0^*/a_T$. It can easily be shown from eqs. [24] and [25] that under these conditions plots of p_{12} and $p_{11} - p_{22}$ as functions of the shear strain γ are temperature invariant.

Both, the shear stress and the primary normal-stress difference run through a maximum before they reach a steady-state. The prediction of the shear stress by using the single exponential damping function (broken line) and by using the experimentally determined damping function (full line) is quite satisfactory. There is only a slight difference between both curves. In the case of $p_{11} - p_{22}$ the position of the maximum as well as the steady-state value depend on the special form of the damping function [7]).

From eqs. [24] and [25] the position of the maximum of p_{12} and $p_{11} - p_{22}$ as well can be obtained. A comparison of the predicted positions and heights of the maxima with the measured quantities is an additional test for the validity of the theory. By differentiating [24] with respect to the time t and using [22] we obtain the following equation for the time t^* of the p_{12} maximum:

$$f_1 \exp[-n_1 \dot{\gamma}_0 t^*](1 - n_1 \dot{\gamma}_0 t^*) + f_2 \exp[-n_2 \dot{\gamma}_0 t^*](1 - n_2 \dot{\gamma}_0 t^*) = 0\,. \quad [29]$$

From [25] the corresponding equation for the time t_0^* of the $p_{11} - p_{22}$ maximum is derived:

[7]) The measured values of $p_{11} - p_{22}$ show a delay in time at the beginning of steady shear flow compared with the predicted behaviour. This delay is mainly caused by an increase of the cone-and-plate gap due to normal forces which must be compensated by a radial flow of the melt (21). To avoid this difficulty the short time behaviour of $p_{11} - p_{22}$ should be compared with flow birefringence measurements (18).

$$f_1 \exp[-n_1 \dot{\gamma}_0 t^*_\Theta]\left(1 - \frac{n_1}{2}\dot{\gamma}_0 t^*_\Theta\right) + f_2 \exp[-n_2 \dot{\gamma}_0 t^*_\Theta]\left(1 - \frac{n_2}{2}\dot{\gamma}_0 t^*_\Theta\right) = 0\,. \quad [30]$$

According to the theory independent of the shear rate $\dot{\gamma}_0$ the maximum of p_{12} is expected at a constant shear strain γ^*, while the maximum of $p_{11} - p_{22}$ is expected at a constant shear strain γ^*_Θ. Using the constants of table 2 the solutions of [29] and [30] are

$$\dot{\gamma}_0 t^* = \gamma^* \approx 6.12 \quad \text{and} \quad \dot{\gamma}_0 t^*_\Theta = \gamma^*_\Theta \approx 17.7. \quad [31]$$

For the single exponential damping function the predicted positions of the maxima (3) are

$$\gamma^* = \frac{\gamma^*_\Theta}{2} = \frac{1}{n} \approx 5.56\,. \quad [32]$$

The experimentally determined damping function predicts the positions of the maxima of p_{12} and $p_{11} - p_{22}$ to differ by about a factor of 3, whereas a factor of 2 should be found according to [32] for the single exponential damping function. As is seen from figure 8 the maxima of the stresses are rather flat. This is why γ^* and γ^*_Θ can only be determined with poor accuracy. Yet it can be said that the description of the measured behaviour by [31] is more realistic compared with [32].

A comparison of the predicted heights of the maxima with measurements is shown in figure 9. By substituting t^* and t^*_Θ for t in [24] and [25], respectively, the viscosity $\eta_{max}(\dot{\gamma}_0)$ and the primary normal stress coefficient $\Theta_{max}(\dot{\gamma}_0)$ in the maxima of the time dependent stresses were calculated. Although the predicted positions of the maxima are sensitive to the special form of the damping function the computed values η_{max} and Θ_{max} are only slightly different. It is also seen from figure 9 that the predicted heights of the maxima agree well with the experimental data.

5.2. Stress relaxation after stop of steady shear flow

In stressing tests the shear stress and the primary normal stress difference reach constant values with time (see fig. 8). If the shear rate is set to zero after the measuring quantities have reached their steady-state, the stresses gradually decrease to zero. The time dependence of the relaxation is denoted by $\tilde{p}_{12}(t; \dot{\gamma}_0)$ and $[\tilde{p}_{11} - \tilde{p}_{22}](t; \dot{\gamma}_0)$. The shear history is defined by

$$\gamma_{t,t'} = \begin{cases} 0 & \text{for} \quad t - t' < t \\ \dot{\gamma}_0(t - t') - \dot{\gamma}_0 t & \text{for} \quad t - t' \geq t\,. \end{cases} \quad [33]$$

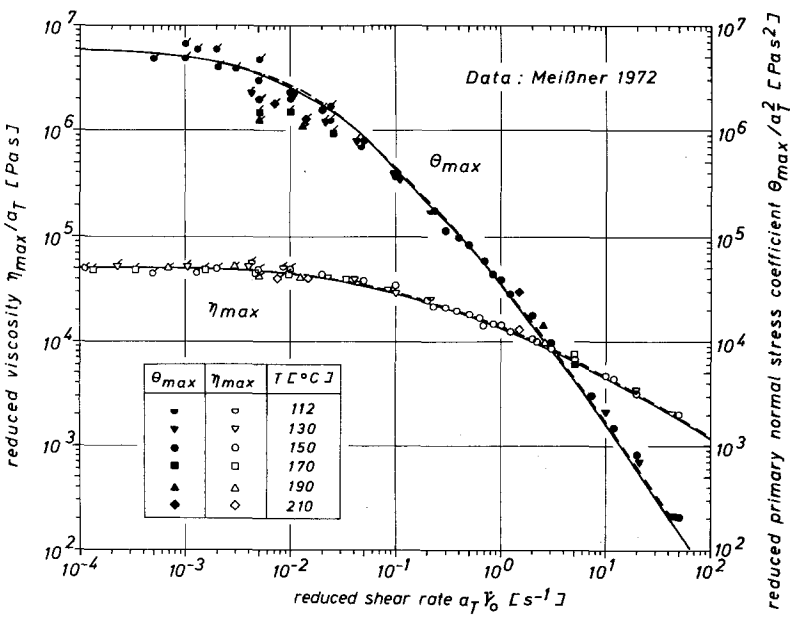

Fig. 9. Temperature invariant representation of the viscosity and primary normal stress coefficient as determined from the maxima of the time dependent stresses in stressing tests. (——) prediction using [17], (– – –) prediction using [18]. The tic denotes steady-state values measured at low shear rates where no maxima occur

In [33] t stands for the time after stop of steady shear flow. By substituting $\gamma_{t,t'}$ in [20] and [21] one obtains

$$\tilde{\eta}(t;\dot{\gamma}_0) = \frac{\tilde{p}_{12}(t;\dot{\gamma}_0)}{\dot{\gamma}_0} = \sum_i \frac{a_i \tau_i^2 \exp[-t/\tau_i]}{(1 + n\dot{\gamma}_0 \tau_i)^2}, \quad [34]$$

$$\tilde{\Theta}(t;\dot{\gamma}_0) = \frac{[\tilde{p}_{11} - \tilde{p}_{22}](t;\dot{\gamma}_0)}{\dot{\gamma}_0^2} = 2\sum_i \frac{a_i \tau_i^3 \exp[-t/\tau_i]}{(1 + n\dot{\gamma}_0 \tau_i)^3}. \quad [35]$$

The relaxation of the shear stress and the primary normal stress difference measured after the stressing tests represented in figure 8 is shown in figure 10.

The stress decay is plotted as a function of the reduced time t/a_T to get temperature invariant curves. The relaxation behaviour as calculated by means of the single exponential damping function (eq. [17]) and the experimentally determined damping function (eq. [18]) is represented in figure 10 by broken and full lines, respectively. The predicted time dependence of the primary normal stress is more sensitive to the special form of the damping function than that of the shear stress. There is a deviation of the experimental data from the calculated behaviour at long times which might be due to experimental error. The oscillations of the calculated curves are caused by the chosen decimal spacing of the τ_i, as discussed above.

6. Conclusion

The comparison of some calculated and measured material functions of Melt I shows that the transient and steady-state shear behaviour is predicted correctly by the theory. The applicability of the constitutive equation to a description of creep and retardation measurements is discussed in (19). The rheological behaviour of the melt in shear is completely characterized by the generalized memory function. The nonlinearity of the rheological behaviour is introduced by the so-called damping function (3, 4) which can directly be determined from measurements of the shear relaxation modulus.

To simplify mathematics the generalized memory function has been approximated by exponential functions. This representation has the advantage that important material functions such as the viscosity function and the primary normal stress function can be calculated by closed integration. Moreover, the derivation of general relations between the different material functions is simplified.

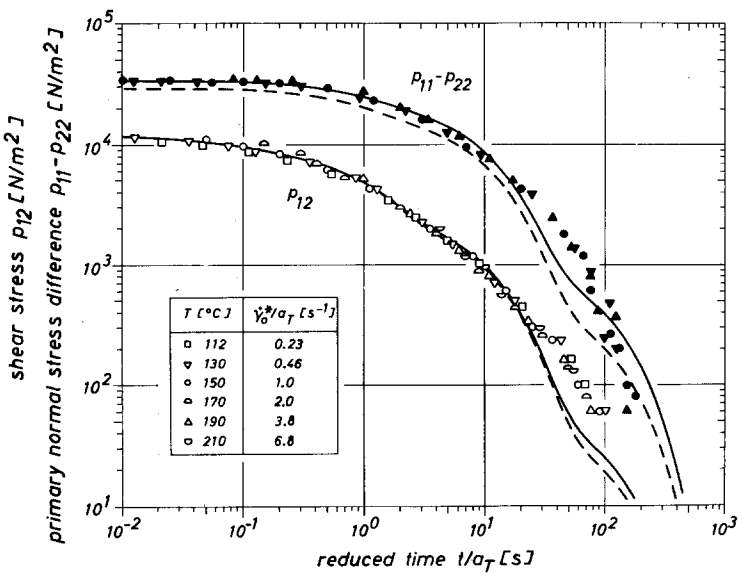

Fig. 10. Time dependence of the relaxation behaviour of the shear stress and the primary normal stress difference from the steady-state of the stressing tests represented in figure 8. (——) prediction using the experimentally determined damping function, (– – –) calculated by means of the single exponential damping function

The constitutive equation presented in this paper gives a realistic description of the linear and nonlinear viscoelastic behaviour of the melt which is mathematically simple enough for use in engineering applications. In plastics processing not only shear deformations but also an elongation of the melt has to be considered. A preliminary application of the theory to the elongational behaviour of Melt I appears very encouraging (3, 20).

Appendix: Relaxation behaviour after steady shear flow of duration Δt

A generalized shear history for relaxation measurements as shown in figure 11 is defined by

$$\gamma_{t,t'} = \begin{cases} 0 & \text{for} \quad t - t' < t \\ \dot\gamma_0 (t - t') - \dot\gamma_0 t & \text{for} \quad t \le t - t' < t + \Delta t \\ \gamma_0 = \dot\gamma_0 \Delta t & \text{for} \quad t - t' \ge t + \Delta t \,. \end{cases} \qquad [36]$$

By substituting $\gamma_{t,t'}$ in [20] one obtains by closed integration

$$p_{12}(t) = \dot\gamma_0 \exp[n\dot\gamma_0 t] \sum_i \frac{a_i \exp\left[-\left(\frac{1}{\tau_i} + n\dot\gamma_0\right)t\right]}{\left(\frac{1}{\tau_i} + n\dot\gamma_0\right)^2} \cdot \left\{1 - \exp\left[-\left(\frac{1}{\tau_i} + n\dot\gamma_0\right)\Delta t\right] \cdot \left[1 + \left(\frac{1}{\tau_i} + n\dot\gamma_0\right)\Delta t\right]\right\} + \dot\gamma_0 \Delta t \sum_i a_i \tau_i \cdot \exp[-t/\tau_i] \exp\left[-\left(\frac{1}{\tau_i} + n\dot\gamma_0\right)\Delta t\right], \qquad [37]$$

which may be written in the form

$$p_{12}(t) = \dot\gamma_0 \sum_i \frac{a_i \tau_i^2 \exp[-t/\tau_i]}{(1 + n\dot\gamma_0 \tau_i)^2} \cdot \left\{1 - \exp\left[-(1 + n\dot\gamma_0 \tau_i)\frac{\Delta t}{\tau_i}\right] \cdot [1 - n\dot\gamma_0 \Delta t (1 + n\dot\gamma_0 \tau_i)]\right\}. \qquad [38]$$

Eq. [38] is valid for the relaxation of the shear stress after a stressing test at a shear rate $\dot\gamma_0$ and duration Δt. The limiting case of [38] for $\Delta t \to \infty$, which corresponds to the relaxation from the steady-state of shear flow, is given by [34].

From eq. [38] one derives the expression

$$p_{12}(t) = \gamma_0 \exp[-n\gamma_0] \sum_i a_i \tau_i \exp\left[-\frac{t + \Delta t}{\tau_i}\right] \cdot \left\{1 + \frac{\Delta t}{2\tau_i} + \frac{\Delta t}{\tau_i} \sum_{k=3}^{\infty} \frac{1}{k!}\left(\frac{\Delta t}{\tau_i} + n\gamma_0\right)^{k-2}\right\} \qquad [39]$$

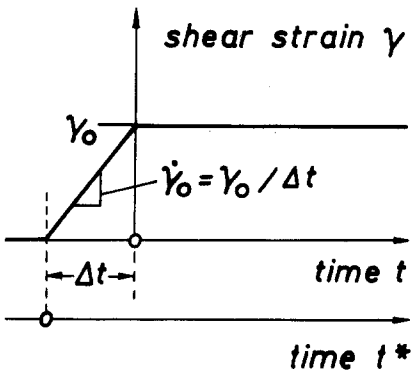

Fig. 11. Shear history for a generalized relaxation experiment

which makes it possible to describe the relaxation modulus for a non-zero rise time Δt. The limiting case for $\Delta t \to 0$ is given by [15].

By substituting [36] in [21] one obtains

$$[p_{11} - p_{22}](t) = \dot\gamma_0^2 2 \sum_i \frac{a_i \tau_i^3 \exp[-t/\tau_i]}{(1 + n\dot\gamma_0 \tau_i)^3} \cdot \left\{1 - \exp\left[-(1 + n\dot\gamma_0 \tau_i)\frac{\Delta t}{\tau_i}\right] \cdot \left[1 + (1 + n\dot\gamma_0 \tau_i)\frac{\Delta t}{\tau_i} - \frac{n\dot\gamma_0 \tau_i}{2}(1 + n\dot\gamma_0 \tau_i)^2 \frac{\Delta t^2}{\tau_i^2}\right]\right\} \qquad [40]$$

which may be written in the form

$$[p_{11} - p_{22}](t) = \gamma_0^2 \exp[-n\gamma_0] \sum_i a_i \tau_i \exp\left[-\frac{t + \Delta t}{\tau_i}\right] \cdot \left\{1 + \frac{\Delta t}{3\tau_i} + 2\frac{\Delta t}{\tau_i} \sum_{k=4}^{\infty} \frac{1}{k!}\left(\frac{\Delta t}{\tau_i} + n\gamma_0\right)^{k-3}\right\}. \qquad [41]$$

The limiting case of [40] for $\Delta t \to \infty$ is given by [35], the limiting case of [41] for $\Delta t \to 0$ by [16].

The influence of a non-zero rise time on the measurements of the shear relaxation modulus is demonstrated in figure 12 for a constant shear strain $\gamma_0 \cdot p_{12}$, which for $\gamma_0 = 1$ is equal to the modulus, is plotted as a function of the total time of test $t^* = \Delta t + t$. The time dependence of p_{12} during the step was calculated by means of [24] using $\dot\gamma_0 = \gamma_0 / \Delta t$. The relaxation behaviour of p_{12} after stop of steady shear was calculated by means of [38]. It is clearly seen from figure 12 that the shear stress increases with Δt if its value is compared at a constant time t^*. For $t^* \gg \Delta t$, however, the influence of the non-zero rise time becomes negligible.

This effect may be taken into account by introducing factors $f(t^*; \gamma_0; \Delta t)$ and $f_\Theta(t^*; \gamma_0; \Delta t)$:

$$G(t^*; \gamma_0; \Delta t) = f(t^*; \gamma_0; \Delta t)\, G(t^*; \gamma_0)\,, \qquad [42]$$

$$G_\Theta(t^*; \gamma_0; \Delta t) = f_\Theta(t^*; \gamma_0; \Delta t)\, G_\Theta(t^*; \gamma_0)\,. \qquad [43]$$

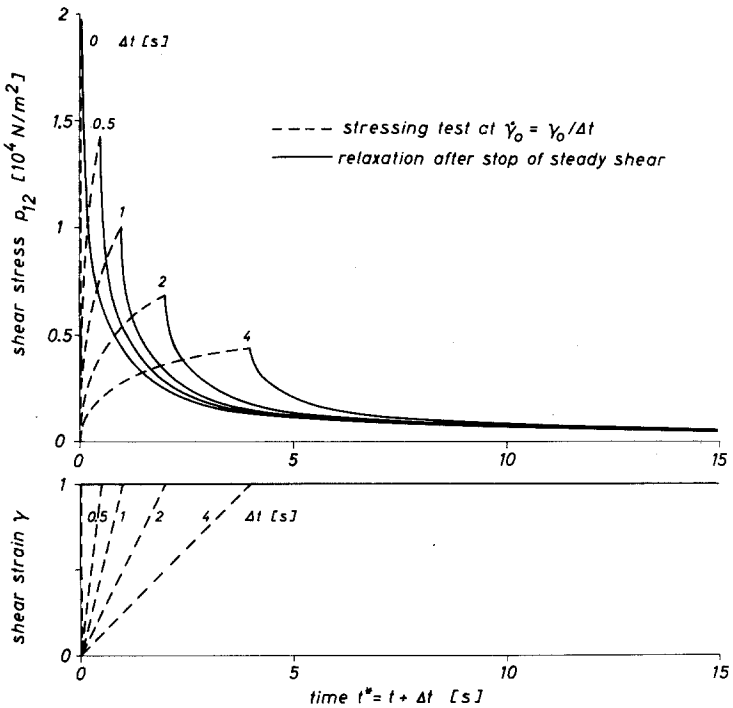

Fig. 12. Calculated time dependence of the shear stress in relaxation measurements at a constant shear strain of $\gamma_0 = 1$ and $T = 150\,°C$ as obtained for different rise times Δt

The quantities on the left hand sides of eqs. [42] and [43] are the directly measured uncorrected moduli $G(t^*; \gamma_0; \Delta t)$ and $G_\Theta(t^*; \gamma_0; \Delta t)$. By means of [39], [41], and [16] the factors f and f_Θ can be calculated as

$$f(t^*; \gamma_0; \Delta t) = \frac{\sum_i a_i \tau_i \exp[-t^*/\tau_i] \left\{1 + \frac{\Delta t}{2\tau_i} + \frac{\Delta t}{\tau_i} \sum_{k=3}^{\infty} \frac{1}{k!} \left(\frac{\Delta t}{\tau_i} + n\gamma_0\right)^{k-2}\right\}}{\sum_i a_i \tau_i \exp[-t^*/\tau_i]}, \qquad [44]$$

$$f_\Theta(t^*; \gamma_0; \Delta t) = \frac{\sum_i a_i \tau_i \exp[-t^*/\tau_i] \left\{1 + \frac{\Delta t}{3\tau_i} + 2\frac{\Delta t}{\tau_i} \sum_{k=4}^{\infty} \frac{1}{k!} \left(\frac{\Delta t}{\tau_i} + n\gamma_0\right)^{k-3}\right\}}{\sum_i a_i \tau_i \exp[-t^*/\tau_i]}. \qquad [45]$$

The directly measured uncorrected moduli were used to determine a first approximation of the damping function $h(\gamma_0)$. By means of relations [42], [44], and [43], respectively, the influence of $st \neq 0$ was taken into account. From the corrected moduli which are plotted in figure 5 the damping function of figure 6 was obtained.

Acknowledgements

The author wishes to express his gratitude to Dr. *H. Münstedt* for helpful comments and to Dr. *M. H. Wagner* for valuable discussions. He is indebted to *R. Benz* and *M. Reuther* for their help in evaluating the experimental data.

Summary

The applicability of a single integral constitutive equation with strain dependent memory function for the description of the nonlinear shear behaviour of a LDPE melt is examined. The generalized memory function is expressed as a product of Lodge's rubberlike-liquid memory function $\dot{\mu}(t - t')$ and a damping function $h(\gamma_{t,t'})$. $\dot{\mu}$ characterizes the time dependence of the linear viscoelastic behaviour and is determined by measurements of the frequency dependence of the complex shear modulus. The damping function describes the nonlinearity of the shear behaviour and can directly be determined by measurements of the shear relaxation modulus. From the temperature invariance of the damping function it follows that also in the nonlinear range a variation of temperature only corresponds to a shift in time scale which can be described by the shift factor $a_T(T)$.

By means of the experimentally determined memory function the shear viscosity and the primary normal stress coefficient as functions of shear rate and temperature can be predicted. The time dependence of the shear stress and of the primary normal stress difference in stressing tests and the relaxation behaviour is described correctly.

Zusammenfassung

Es wird die Anwendbarkeit einer Zustandsgleichung vom Integraltyp nach *Lodge* mit einer deformationsabhängigen Gedächtnisfunktion zur Beschreibung des nichtlinearen Scherfließens einer LDPE-Schmelze untersucht. Die verallgemeinerte Gedächtnisfunktion wird als Produkt der Gedächtnisfunktion des linearen Verhaltens $\mathring{\mu}(t-t')$ und einer Dämpfungsfunktion $h(\gamma_{t,t'})$ dargestellt. $\mathring{\mu}$ charakterisiert die Zeitabhängigkeit des viskoelastischen Verhaltens und wird aus Messungen der Frequenzabhängigkeit des komplexen Schubmoduls bestimmt. Die Dämpfungsfunktion beschreibt die Nichtlinearität des Scherverhaltens und ist über Messungen des Relaxationsmoduls direkt meßbar. Die Temperaturunabhängigkeit der Dämpfungsfunktion hat zur Folge, daß auch im nichtlinearen Fließbereich eine Temperaturänderung nur einer Verschiebung der Zeitskala entspricht, die durch den Verschiebungsfaktor $a_T(T)$ beschrieben werden kann.

Die experimentell ermittelte Gedächtnisfunktion erlaubt die Voraussage des Verlaufs der Viskosität und des ersten Normalspannungskoeffizienten in Abhängigkeit von der Schergeschwindigkeit und der Temperatur. Ebenso werden die Zeitabhängigkeit der Schubspannung und der ersten Normalspannungsdifferenz im Spannversuch und das Relaxationsverhalten richtig beschrieben.

References

1) *Lodge, A. S.*, Elastic Liquids (London-New York 1964).

2) *Lodge, A. S.*, Body Tensor Fields in Continuum Mechanics (London-New York 1974).

3) *Wagner, M. H.*, Rheol. Acta **15**, 136 (1976).

4) *Wagner, M. H.*, Rheol. Acta **16**, 43 (1977).

5) *Meissner, M.*, J. Appl. Polymer Sci. **16**, 2877 (1972).

6) *Meissner, M.*, Rheol. Acta **14**, 201 (1975).

7) *Meissner, M.*, Rheol. Acta **10**, 230 (1971).

8) *Meissner, M.*, Rheol. Acta **14**, 471 (1975).

9) *Chang, Hui, A. S. Lodge*, Rheol. Acta **11**, 127 (1972).

10) *Zosel, A.*, private communication.

11) *Ferry, J. D.*, Viscoelastic Properties of Polymers (New York 1970).

12) *Meissner, J.*, In: *G. Schreyer*, Konstruieren mit Kunststoffen (Carl Hanser Verlag, München 1972).

13) *Schwarzl, F., A. J. Stavermann*, J. Appl. Phys. **23**, 838 (1952).

14) *Osaki, K.*, Proc. VIIth Int. Congr. Rheology **104** (Gothenburg Sweden 1976).

15) *Fukuda, M., K. Osaki, M. Kurata*, J. Polym. Sci., Physics **13**, 1563 (1975).

16) *Vinogradov, G. V., A. Ya. Malkin*, J. Polym. Sci. A-2, **4**, 135 (1966).

17) *Vinogradov, G. V., A. Ya. Malkin*, J. Polym. Sci. A-2, **2**, 2357 (1964).

18) *Gortemaker, F. H., M. G. Hansen, B. de Cindio, H. M. Laun, H. Janeschitz-Kriegl*, Rheol. Acta **15**, 256 (1976).

19) *Wagner, M. H., H. M. Laun*, submitted to Rheol. Acta.

20) *Wagner, M. H.*, Rheol. Acta **15**, 133 (1976).

21) *Walters, K.*, Rheometry (Chapman and Hall, London 1975).

22) *Phillips, M. C.*, Proc. Conference 'Polymer Rheology and Plastics Processing', Loughborough, U.K. (1975).

23) *Gleissle, W.*, Rheol. Acta **15**, 305 (1976).

24) *Bernstein, B., E. A. Kearsly, L. J. Zapas*, Trans. Soc. Rheol. **8**, 391 (1963).

Author's address:

Dr. *H. M. Laun*
Meß- und Prüflaboratorium
BASF Aktiengesellschaft
D-6700 Ludwigshafen (BRD)